The effect of mixed alkalis on the absorption and fluorescence properties of Ho^{3+} ions in borate glasses

The effect of mixed alkalis on the absorption and fluorescence properties of Ho^{3+} ions in borate glasses

Y C Ratnakaram[1,3]**, D Thirupathi Naidu**[1]**, A Vijaya Kumar**[1] **and J L Rao**[2]

[1] SV University PG Centre, Kavali-524201, AP, India
[2] SV University, Tirupathi-517402, AP, India

E-mail: ratnakaram_yc@yahoo.co.in

Abstract

Spectroscopic properties of Ho^{3+} in $67B_2O_3 \cdot xLi_2O \cdot (32 - x)Na_2O$, $67B_2O_3 \cdot xLi_2O \cdot (32 - x)K_2O$ and $67B_2O_3 \cdot xLi_2O \cdot (32 - x)Cs_2O$ (where $x = 8$, 12, 16, 20 and 24) glasses were investigated on the basis of Judd–Ofelt theory. Various spectroscopic parameters (E^1, E^2, E^3, ξ_{4f}, α and β) and Judd–Ofelt intensity parameters (Ω_2, Ω_4 and Ω_6) are calculated as a function of x in the three glass matrices. The obtained Judd–Ofelt intensity parameter Ω_2 increases with the addition of a second alkali and also shows minima or maxima at $x = 16$–20 mol% in the above glasses. Using Judd–Ofelt intensity parameters (Ω_2, Ω_4 and Ω_6), radiative transition probabilities (A_T), radiative lifetimes (τ_R), branching ratios (β) and integrated absorption cross sections (Σ) have been calculated for certain excited states of Ho^{3+}. The non-radiative transition rates of different excited states of Ho^{3+} are also estimated from 'energy gap law'. From the luminescence spectra, stimulated emission cross-sections (σ_p) have been obtained for the two transitions $^5F_5 \rightarrow {}^5I_8$ and $^3K_8 \rightarrow {}^5I_8$ of Ho^{3+}. The trend of all these parameters observed as a function of x in these glass systems have been discussed, keeping in mind the effect of mixed alkalis.

1. Introduction

Glasses doped with rare earth ions have been used as a material for high power lasers. Radiative transitions between 4f levels of rare earth ions have been applied for various optical devices such as high power glass lasers, infrared-excitable phosphors, optical amplifiers and so on. Recent interest in the development of solid state lasers for radiation at a wavelength of 3 μm has been stimulated by requirements for medical applications [1]. Ho^{3+} ions can produce laser emission in the 2 and 2.9 μm ranges [2–4] arising from transitions between Stark levels of the

---

[3] Author to whom any correspondence should be addressed.

$^5I_7$ and $^5I_6$ states, respectively, and the $^5I_8$ ground state. Malinowski *et al* [5] reported the optical transitions of Ho^{3+} in YAG crystal. Judd–Ofelt parameters and multi-phonon relaxations of Ho^{3+} ions in $ZnCl_2$ based glass were studied by Shojiya *et al* [6]. Optical absorption and fluorescence spectral studies of Ho^{3+} ions in PbO–Al_2O_3–B_2O_3 glass system were analysed by Reddy *et al* [7]. Previously, the authors have investigated the optical properties of Ho^{3+} doped $70B_2O_3 \cdot xNa_2O \cdot (30 - x)K_2O$ glasses [8].

All the properties of glasses, which are strongly affected by the long range motion of ions, show large deviation from a simple additive behaviour upon mixing of two different types of mobile ions. This phenomenon is known as the 'mixed alkali effect' [9]. Recent progress in understanding the mixed alkali effect has been initiated by the development of the dynamic structure model [9, 10]. The effect of mixed alkalis on most glass properties has been extensively investigated and reviewed in several articles [10–12]. In mixed alkali borate glasses, the B_2O_3 is assumed to consist of boroxyl rings and BO_3 triangles and constitutes a random network composed of two-dimensional units. The existence of several structural groups containing both three and four co-ordinated boron was first postulated by Krogh-Moe [13] and confirmed by comparison with IR spectra of crystalline sodium borate compounds. Chong *et al* [14] showed that mixed alkali borate glasses have structures that are quite similar to the binary borate glasses.

The present work aims at analysing the results of systematic studies on Ho^{3+} ions in $67B_2O_3 \cdot xLi_2O \cdot (32-x)Na_2O$, $67B_2O_3 \cdot xLi_2O \cdot (32-x)K_2O$ and $67B_2O_3 \cdot xLi_2O \cdot (32-x)Cs_2O$ (where $x = 8, 12, 16, 20$ and 24) glasses, keeping in mind the effect of mixed alkalis on the optical properties of Ho^{3+} in these glasses. Various spectroscopic parameters like Racah (E^1, E^2 and E^3), spin–orbit (ξ_{4f}) and configuration interaction (α, β) parameters are deduced as a function of x. Energy values and spectral intensities of different excited states are calculated as a function of x. Radiative and non-radiative transition rates (A_T and W_{MPR}), radiative lifetimes (τ_R), branching ratios (β) and integrated absorption cross sections (Σ) are calculated for certain excited states of Ho^{3+} in these borate glasses. From the emission spectra, peak wavelengths (λ_p), effective line widths ($\Delta\lambda_{eff}$) and emission cross sections (σ_p) have been obtained for certain transitions. From the magnitudes of branching ratios and cross sections, certain transitions are identified for lasing action.

2. Experimental details

The glasses were prepared in the laboratory using the method described in a previous paper [15]. Optical absorption measurements were made using a Hitachi U-3400 spectrophotometer. Photoluminescence spectra were obtained for lithium sodium and lithium potassium mixed alkali borate glasses using a Hitachi U-4700 spectrophotometer under a excitation wavelength of 418 nm. The density of the samples was measured by the Archimedes principle using xylene as the immersion liquid with an accuracy of ± 0.005 g cm^{-3}. The glass refractive indices were measured with an Abbe refractometer with an accuracy of ± 0.001. The glass systems studied in the present work are $67B_2O_3 \cdot xLi_2O \cdot (32 - x)Na_2O$ (LSG), $67B_2O_3 \cdot xLi_2O \cdot (32 - x)K_2O$ (LPG) and $67B_2O_3 \cdot xLi_2O \cdot (32 - x)Cs_2O$ (LCG) (where $x = 8, 12, 16, 20$ and 24) and are detailed below.

<div align="center">

Glass 1—H_3BO_3:Li_2CO_3:Na_2CO_3:$Ho_2O_3 = 67:8:24:1$

Glass 2—H_3BO_3:Li_2CO_3:Na_2CO_3:$Ho_2O_3 = 67:12:20:1$

Glass 3—H_3BO_3:Li_2CO_3:Na_2CO_3:$Ho_2O_3 = 67:16:16:1$

Glass 4—H_3BO_3:Li_2CO_3:Na_2CO_3:$Ho_2O_3 = 67:20:12:1$

Glass 5—H_3BO_3:Li_2CO_3:Na_2CO_3:$Ho_2O_3 = 67:24:8:1$

</div>

Glass 6—H$_3$BO$_3$:Li$_2$CO$_3$:K$_2$CO$_3$:Ho$_2$O$_3$ = 67:8:24:1
Glass 7—H$_3$BO$_3$:Li$_2$CO$_3$:K$_2$CO$_3$:Ho$_2$O$_3$ = 67:12:20:1
Glass 8—H$_3$BO$_3$:Li$_2$CO$_3$:K$_2$CO$_3$:Ho$_2$O$_3$ = 67:16:16:1
Glass 9—H$_3$BO$_3$:Li$_2$CO$_3$:K$_2$CO$_3$:Ho$_2$O$_3$ = 67:20:12:1
Glass 10—H$_3$BO$_3$:Li$_2$CO$_3$:K$_2$CO$_3$:Ho$_2$O$_3$ = 67:24:8:1

Glass 11—H$_3$BO$_3$:Li$_2$CO$_3$:Cs$_2$CO$_3$:Ho$_2$O$_3$ = 67:8:24:1
Glass 12—H$_3$BO$_3$:Li$_2$CO$_3$:Cs$_2$CO$_3$:Ho$_2$O$_3$ = 67:12:20:1
Glass 13—H$_3$BO$_3$:Li$_2$CO$_3$:Cs$_2$CO$_3$:Ho$_2$O$_3$ = 67:16:16:1
Glass 14—H$_3$BO$_3$:Li$_2$CO$_3$:Cs$_2$CO$_3$:Ho$_2$O$_3$ = 67:20:12:1
Glass 15—H$_3$BO$_3$:Li$_2$CO$_3$:Cs$_2$CO$_3$:Ho$_2$O$_3$ = 67:24:8:1

3. Results and analysis

3.1. Spectroscopic parameters

The optical absorption spectra of Ho^{3+} doped lithium sodium mixed alkali borate glasses are shown in figure 1. The absorption spectra of Ho^{3+} in lithium potassium and lithium caesium mixed alkali borate glasses are not shown as they are a similar shape. The transitions were assigned by comparing the band positions in the absorption spectrum with an energy level scheme of LaF$_3$:Ho^{3+}, published by Carnall *et al* [16]. Using the observed band energies as E_J, zero point energies (E_{0J}) and partial derivatives, the correction factors ΔE_J, $\Delta\xi_{4f}$, $\Delta\alpha$ and $\Delta\beta$ have been evaluated by the least squares fit method. The rms deviation between the energies calculated with these parameters and the experimental energies are zero for all the glass systems except for three which have very small deviations and observed that a full matrix diagonalization procedure leads to a good fit between the experimental and calculated energies. The Racah (E^1, E^2 and E^3), spin–orbit (ξ_{4f}), configuration interaction (α, β) parameters and hydrogenic ratios ((E^1/E^3) and (E^2/E^3)) for all the glasses studied are presented in table 1. The experimental oscillator strength, f_{exp}, of the electric dipole transition is obtained from [16]

$$f_{exp} = 4.32 \times 10^{-9} \int \in(\nu)\,d\nu \tag{1}$$

where $\in(\nu)$ is the molar absorptivity of a band at mean energy ν (cm^{-1}) and may be computed from the measured absorbance A, for known concentrations of the Ho^{3+} ions and the thickness of the sample. In the present work, the intensities of all the absorption bands have been measured using the area method. The theoretical oscillator strength, f_{cal}, of electric dipole transitions within f^N configurations can be calculated using Judd–Ofelt theory [17, 18] in terms of three intensity parameters Ω_2, Ω_4 and Ω_6 using the relation

$$f_{cal}(aJ, bJ') = \frac{8\Pi^2 mc\nu}{3h(2J+1)} \frac{(n^2+2)^2}{9n} \sum_{\lambda=2,4,6} \Omega_\lambda \|\langle(SL)J\|U^\lambda\|(S'L')J'\rangle\|^2 \tag{2}$$

Ω_λ can be also written as

$$\Omega_\lambda = (2t+1)\sum_{t,p} |A_{t,p}|^2 \Xi^2(t,\lambda)(2s+1)^{-1}, \qquad t = 2, 4, 6 \tag{3}$$

where $A_{t,p}$ are components of the crystal field operator and depend on the symmetry of the crystal field around Ho^{3+} ions and $\Xi(t,\lambda)$ is a function of radial integral and depends reciprocally on the energy separations of the 4f level and admixing levels, e.g. 5d, 5g. The sum over λ includes only the even values 2, 4 and 6, whereas the sum over t includes only
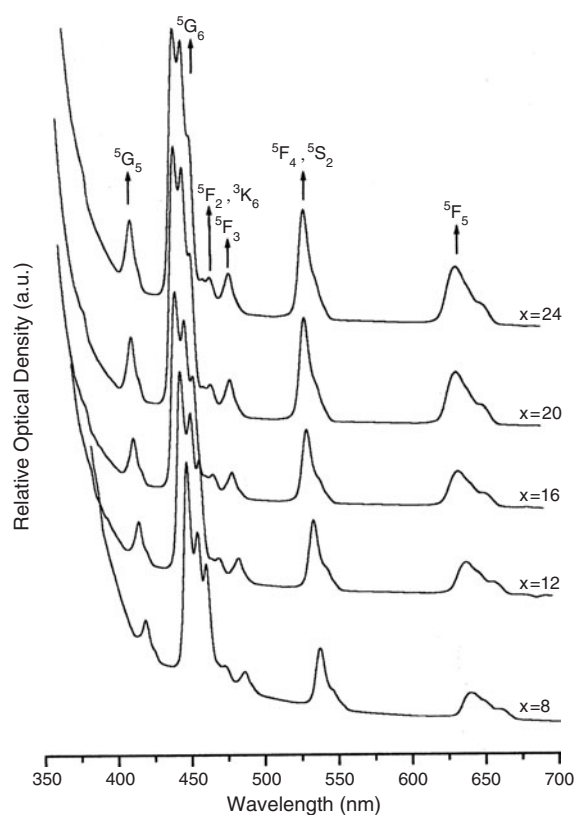
Figure 1. Optical absorption spectra of Ho^{3+} in $67B_2O_3 \cdot xLi_2O \cdot (32 - x)Na_2O$ glasses.

the odd values 1, 3 and 5. It has been suggested by Reisfeld [19] that Ξ is related to the nephelauxetic parameter, β, which indicates the degree of covalency of R–O bonds [20].

In equation (2), m represents electron mass, c the speed of light, h Planck's constant and n is the refractive index of glass. The squared reduced matrix elements of the unit tensor operator, $\|U^\lambda\|^2$, on right-hand side of the equation (2) are taken from the literature [21]. Substituting the 'f_{meas}' for 'f_{cal}' and using the squared reduced matrix elements, the three intensity parameters Ω_2, Ω_4 and Ω_6 are obtained. The three intensity parameters are the characteristics of a given rare earth ion (in a given matrix) and are related to the radial wavefunctions of the states $4f^N$ and the admixing states $4f^{N-1}5d$ or $4f^{N-1}5g$ and the ligand field parameters that characterize the environmental field. Due to the overlapping of the band $^5F_4$ on $^5S_2$ and $^5F_2$ on $^3K_8$, they are treated as two independent single bands with an appropriate combination of the respective reduced matrix elements. The rms deviation (goodness of the fit) between the experimental and calculated oscillator strengths is quite good, which proves the validity of the approximations made in the Judd–Ofelt theory.

In table 2, the Judd–Ofelt intensity parameters (Ω_2, Ω_4 and Ω_6) and the sum of the intensity parameters ($\sum \Omega_\lambda$) of Ho^{3+} in various glass matrices are presented. These parameters depend on the host glass composition [22]. Generally Ω_2 is an indicator of the covalency and Ω_4 and Ω_6 are related to the rigidity of the host matrix. Oomen and van Dongen [23] have suggested that, instead of observing the variation in Ω_2 alone, it is convenient to see the variation of the sum of the Judd–Ofelt parameters $\sum \Omega_\lambda$, which also increase with increasing covalency. From table 2 it is observed that $\sum \Omega_\lambda$ increases, compared to their values in binary sodium borate or potassium borate or lithium borate glasses, when the third component is added. It

Table 1. Various spectroscopic parameters (E^1, E^2, E^3, ξ_{4f}, α and β) and hydrogenic ratios (E^1/E^3 and E^2/E^3) of Ho^{3+} doped mixed alkali borate glasses.

Sample no	Glass composition	E^1	E^2	E^3	ξ_{4f}	α	β	E^1/E^3	E^2/E^3	Reference
1	67B$_2$O$_3$·8Li$_2$O·24Na$_2$O	7448	30.9	720.0	2003.1	141.1	−3925	10.3	0.043	Present work
2	67B$_2$O$_3$·12Li$_2$O·20Na$_2$O	7466	32.2	703.1	2036.0	126.9	−3581	10.6	0.046	Present work
3	67B$_2$O$_3$·16Li$_2$O·16Na$_2$O	7462	33.2	689.2	2055.5	113.6	−3306	10.8	0.048	Present work
4	67B$_2$O$_3$·20Li$_2$O·12Na$_2$O	7284	33.1	676.2	2070.2	94.6	−2782	10.7	0.048	Present work
5	67B$_2$O$_3$·24Li$_2$O·8Na$_2$O	7284	33.1	676.2	2070.2	94.6	−2782	10.7	0.048	Present work
6	67B$_2$O$_3$·8Li$_2$O·24K$_2$O	6788	25.9	724.5	1934.9	118.3	−3183	9.4	0.035	Present work
7	67B$_2$O$_3$·12Li$_2$O·20K$_2$O	7174	28.9	724.5	1957.6	134.3	−3729	9.9	0.040	Present work
8	67B$_2$O$_3$·16Li$_2$O·16K$_2$O	7733	30.9	734.1	1998.4	167.2	−4702	10.5	0.042	Present work
9	67B$_2$O$_3$·20Li$_2$O·12K$_2$O	7419	31.7	704.1	2027.0	125.9	−3581	10.5	0.045	Present work
10	67B$_2$O$_3$·24Li$_2$O·8K$_2$O	7180	31.3	687.1	2043.1	101.6	−2909	10.5	0.045	Present work
11	67B$_2$O$_3$·8Li$_2$O·24Cs$_2$O	7166	30.5	713.3	2007.8	120.9	−3296	10.0	0.043	Present work
12	67B$_2$O$_3$·12Li$_2$O·20Cs$_2$O	7653	32.1	709.0	2034.1	141.7	−4103	10.8	0.045	Present work
13	67B$_2$O$_3$·16Li$_2$O·16Cs$_2$O	7380	31.5	711.1	2018.5	129.8	−3601	10.4	0.044	Present work
14	67B$_2$O$_3$·20Li$_2$O·12Cs$_2$O	7501	31.6	718.9	2029.9	141.9	−3954	10.4	0.044	Present work
15	67B$_2$O$_3$·24Li$_2$O·8Cs$_2$O	7399	32.3	700.3	2052.0	118.9	−3344	10.6	0.046	Present work
16	70B$_2$O$_3$ + 5Na$_2$O + 25K$_2$O	7081	31.4	696.5	2072.2	105.7	−2722	10.16	0.045	[8]
17	70B$_2$O$_3$ + 10Na$_2$O + 20K$_2$O	7205	31.8	703.6	2039.3	115.8	−3128	10.24	0.045	[8]
18	70B$_2$O$_3$ + 15Na$_2$O + 15K$_2$O	7199	32.1	695.4	1990.0	103.8	−3023	10.35	0.046	[8]
19	70B$_2$O$_3$ + 20Na$_2$O + 10K$_2$O	7280	31.1	707.7	1994.5	120.1	−3458	10.30	0.044	[8]
20	70B$_2$O$_3$ + 25Na$_2$O + 5K$_2$O	7359	30.7	717.7	1994.8	133.9	−3172	10.25	0.043	[8]

indicates that covalency increases with the addition of a second alkali in the glass matrix. In the present work, it is observed that the $\sum \Omega_\lambda$ value increases with the increase of x in lithium sodium glass. For lithium potassium glass, $\sum \Omega_\lambda$ increases up to $x = 16$ mol% and decreases for $x = 20$ and 24 mol%. In the case of lithium caesium glass, $\sum \Omega_\lambda$ inflects with x, which indicates structural changes.

The results of earlier studies on borate glasses [24] indicate that in alkali borate glasses, at $x = 15$–20 mol%, the concentration of tetra borate groups is at a maximum and boroxyl groups disappear. From $x = 20$ mol%, formation of diborates takes place. For $x > 30$ mol%, the formation of non-bridging oxygen starts and increases in concentration with the introduction of modifying oxides into the glass forming network. This reduces the average chemical bond strength, leading to a lower covalency. In the present work, it is observed that (from table 2) $\sum \Omega_\lambda$ is minimum for $x = 8$ mol% in all the three glass matrices, which indicates low covalency (high ionicity) between holmium cations and oxygen anions or to a relatively high symmetry of local surrounding of the holmium ion in these glass matrices. $\sum \Omega_\lambda$ is maximum at $x = 24$, 16 and 12 mol% for lithium sodium, lithium potassium and lithium caesium glasses matrices, respectively which indicates higher covalency at these compositions.

For Ho^{3+} ion, $^5I_8 \rightarrow {}^5G_6$ and $^5I_8 \rightarrow {}^3H_6$ are the hypersensitive transitions, which obeys the selection rules $\Delta J \leqslant 2$, $\Delta L \leqslant 2$ and $\Delta S = 0$. The peak positions and the intensities of these transitions are sensitive to the environment of the ion. In the present work, the $^5I_8 \rightarrow {}^3H_6$ transition was not observed. The peak position (nm) of the $^5I_8 \rightarrow {}^5G_6$ transition in different glass matrices are given below.

|					
Glass 1	446.5	Glass 6	446.0	Glass 11	445.0
Glass 2	447.5	Glass 7	446.5	Glass 12	448.0
Glass 3	448.0	Glass 8	447.0	Glass 13	446.5
Glass 4	448.5	Glass 9	447.5	Glass 14	446.0
Glass 5	449.0	Glass 10	448.5	Glass 15	446.0.

Table 2. Judd–Ofelt intensity parameters ($\Omega_\lambda \times 10^{20}$) (cm^2) and peak intensity ratios (I_L/I_S) of hypersensitive transition ($^5G_6$) of Ho^{3+} doped mixed alkali borate glasses.

Sample no	Glass composition	Ω_2	Ω_4	Ω_6	$\sum \Omega_\lambda$	I_L/I_S (2, 1)	Reference
1	$67B_2O_3 \cdot 8Li_2O \cdot 24Na_2O$	11.15	2.64	3.35	17.13	1.130	Present work
2	$67B_2O_3 \cdot 12Li_2O \cdot 20Na_2O$	11.71	3.95	3.85	19.50	1.181	Present work
3	$67B_2O_3 \cdot 16Li_2O \cdot 16Na_2O$	11.91	4.57	4.37	20.86	1.253	Present work
4	$67B_2O_3 \cdot 20Li_2O \cdot 12Na_2O$	11.46	5.09	4.82	21.38	1.311	Present work
5	$67B_2O_3 \cdot 24Li_2O \cdot 8Na_2O$	11.92	5.20	4.87	21.97	1.366	Present work
6	$67B_2O_3 \cdot 8Li_2O \cdot 24K_2O$	7.32	0.55	1.47	9.35	0.985	Present work
7	$67B_2O_3 \cdot 12Li_2O \cdot 20K_2O$	9.95	1.35	2.38	13.68	1.020	Present work
8	$67B_2O_3 \cdot 16Li_2O \cdot 16K_2O$	10.48	2.38	3.05	15.92	1.172	Present work
9	$67B_2O_3 \cdot 20Li_2O \cdot 12K_2O$	9.59	2.76	3.08	15.37	1.287	Present work
10	$67B_2O_3 \cdot 24Li_2O \cdot 8K_2O$	8.19	3.44	3.03	14.65	1.490	Present work
11	$67B_2O_3 \cdot 8Li_2O \cdot 24Cs_2O$	7.47	1.09	1.28	9.84	0.975	Present work
12	$67B_2O_3 \cdot 12Li_2O \cdot 20Cs_2O$	14.07	5.33	4.61	24.01	1.110	Present work
13	$67B_2O_3 \cdot 16Li_2O \cdot 16Cs_2O$	9.31	2.15	2.48	13.94	1.062	Present work
14	$67B_2O_3 \cdot 20Li_2O \cdot 12Cs_2O$	7.77	2.79	2.37	12.93	1.092	Present work
15	$67B_2O_3 \cdot 24Li_2O \cdot 8Cs_2O$	8.79	4.34	2.86	15.99	1.102	Present work
16	$70B_2O_3 + 5Na_2O + 25K_2O$	7.47	0.57	1.23	9.28	1.209	[8]
17	$70B_2O_3 + 10Na_2O + 20K_2O$	12.23	2.43	3.13	17.77	1.815	[8]
18	$70B_2O_3 + 15Na_2O + 15K_2O$	13.55	1.88	3.76	19.20	1.785	[8]
19	$70B_2O_3 + 20Na_2O + 10K_2O$	13.99	2.36	3.04	19.41	1.923	[8]
20	$70B_2O_3 + 25Na_2O + 5K_2O$	13.47	2.05	2.56	18.09	1.766	[8]
21	$30Na_2O + 70B_2O$	5.30	2.52	1.53	9.35		[27]
22	$30K_2O + 70B_2O$	5.29	1.40	0.78	7.47		[27]
23	$30Li_2O + 70B_2O$	4.56	3.14	1.78	9.48		[27]

The shift of peak wavelength of the hypersensitive transition towards longer wavelength with an increase of alkali content indicates that the degree of covalency of the R–O bond increases with alkali content. In the present work, it is observed that there is a shift of peak wavelength of the $^5I_8 \rightarrow {}^5G_6$ transition towards longer wavelengths with x in both lithium sodium and lithium potassium glass matrices which indicates increase in covalency. For the lithium caesium glass matrix, there is a shift of the peak wavelength of the hypersensitive transition towards longer wavelengths, and for $x = 8$–12 mol%, from $x = 12$ to 16 mol%, a shift towards shorter wavelength; further there is no change in the peak wavelength.

The spectral profile of the hypersensitive transition $^5I_8 \rightarrow {}^5G_6$ is shown in figure 2 for the three glass matrices. A difference in shape of this transition indicates a difference in the environment of the Ho^{3+} ion. It indicates changes in the symmetry of the crystalline field acting on the rare earth ion. The hypersensitive transition, $^5I_8 \rightarrow {}^5G_6$, in all the absorption spectra of Ho^{3+} doped glasses is split into three sharp peaks by Stark splitting due to crystal field (peaks 1, 2 and 3 in figure 2). The peak to peak separation is the same in all the mixed alkali borate glasses. As x increases from 8 to 24 mol%, the height of peak 1 decreases and the height of peak 2 increases (relatively) in lithium sodium and lithium potassium mixed alkali borate glasses. In the lithium caesium glass matrix, the shape of the spectral profile is different for $x = 8$ mol% from other compositions. These changes indicate the structural changes around the Ho^{3+} ion in these glass matrices. The relative intensity ratio between the peaks I_L/I_S, where I_L is the intensity of the peak with longer wavelength and I_S is the intensity of the peak with shorter wavelength, varies with glass composition. The peak intensity ratios are
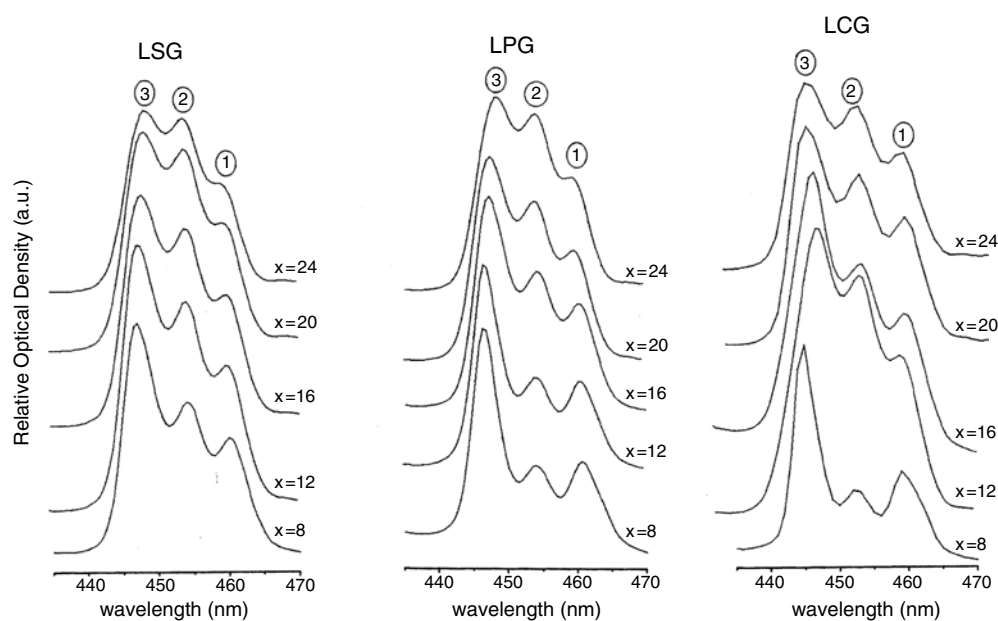
Figure 2. Variation of spectral profiles of hypersensitive transition ($^5I_8 \rightarrow {}^5G_6$) with x in mixed alkali borate glasses.

presented in table 2. From the table it is observed that the I_L/I_S values of the peaks 2 and 1 are increasing with the increase of x in lithium sodium and lithium potassium glass matrices. In the case of lithium caesium glass, the I_L/I_S value inflects with x. An increase in the intensity ratio (I_L/I_S) is found to indicate a shift of the centre of gravity of the absorption spectra to longer wavelengths. This indicates an increase in the covalence of the Ho–O bond.

From the above studies, it is observed that from the variation of the sum of the Judd–Ofelt intensity parameters ($\sum \Omega_\lambda$), the position of the peak wavelength of the hypersensitive transition, peak intensity ratios (I_L/I_S) and from equation (3), covalency increases with the increase of x in the lithium sodium glass matrix. Some structural changes were observed at $x = 20$ and 24 mol% in lithium potassium and lithium caesium glass matrices.

3.2. Radiative and non-radiative properties

According to Judd–Ofelt theory, the Judd–Ofelt intensity parameters and spontaneous emission probabilities are affected by the structural change around rare earth ions and/or the covalency of the rare earth ion sites. The radiative properties are estimated using the formulae given in an earlier paper [8]. Table 3 presents the total radiative transition probabilities (A_T) of $^3H_5$, $^5G_6$, $^3K_8$, $^5F_2$, $^5F_3$, $^5F_4$ and $^5F_5$ states of Ho^{3+} doped different mixed alkali borate glasses. The error in the estimated radiative transition rates is nearly $\pm 10\%$ for all the excited states. The total radiative transition rates for all the excited states are low at $x = 8$ mol% in all the three mixed alkali borate glasses. These values are high at $x = 24$ and at 12 mol% in lithium sodium and lithium caesium glass matrices. The variation of A_T with x is shown in figure 3 for lithium sodium, lithium potassium and lithium caesium glass matrices, respectively.

The calculated branching ratios (β) and integrated absorption cross sections (Σ) of certain transitions of Ho^{3+} ion can be observed in table 4. These values show that the magnitude of branching ratios are high at $x = 8$ mol% for most of the transitions in all the three glass matrices and the integrated absorption cross section is high for the $^5G_6 \rightarrow {}^5I_8$ transition among all the
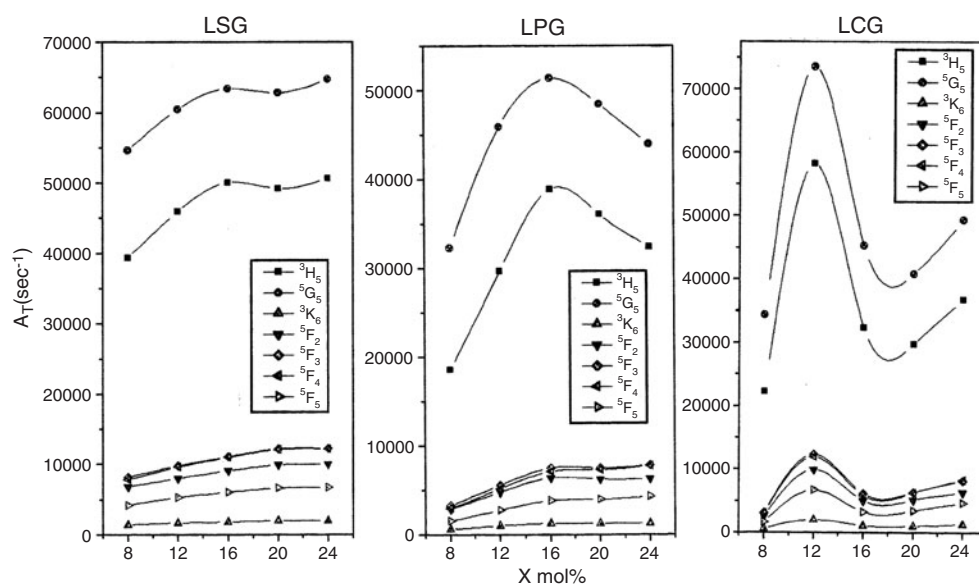
Figure 3. Variation of A_T with x in lithium sodium (LSG), lithium potassium (LPG) and lithium caesium (LCG) mixed alkali borate glasses.

Table 3. Total radiative transition probabilities (A_T) (s^{-1}) of certain excited states of Ho^{3+} in mixed alkali borate glasses.

Sample no	Glass composition	$^3H_5$	$^5G_6$	$^3K_8$	$^5F_2$	$^5F_3$	$^5F_4$	$^5F_5$
1	$67B_2O_3 \cdot 8Li_2O \cdot 24Na_2O$	39 351	54 638	1430	6 860	8 159	7 802	4238
2	$67B_2O_3 \cdot 12Li_2O \cdot 20Na_2O$	45 946	60 470	1678	8 007	9 782	9 611	5294
3	$67B_2O_3 \cdot 16Li_2O \cdot 16Na_2O$	50 122	63 417	1881	9 107	11 158	11 037	6069
4	$67B_2O_3 \cdot 20Li_2O \cdot 12Na_2O$	49 271	62 847	2026	9 910	12 211	12 111	6641
5	$67B_2O_3 \cdot 24Li_2O \cdot 8Na_2O$	50 687	64 784	2056	10 000	12 337	12 248	6725
6	$67B_2O_3 \cdot 8Li_2O \cdot 24K_2O$	18 653	32 303	677	2 911	3 312	2 996	1595
7	$67B_2O_3 \cdot 12Li_2O \cdot 20K_2O$	29 698	45 915	1051	4 816	5 596	5 210	2806
8	$67B_2O_3 \cdot 16Li_2O \cdot 16K_2O$	38 887	51 417	1317	6 385	7 524	7 172	3899
9	$67B_2O_3 \cdot 20Li_2O \cdot 12K_2O$	36 141	48 466	1315	6 270	7 567	7 353	4022
10	$67B_2O_3 \cdot 24Li_2O \cdot 8K_2O$	32 428	44 004	1313	6 356	7 874	7 799	4323
11	$67B_2O_3 \cdot 8Li_2O \cdot 24Cs_2O$	22 350	34 392	663	2 636	3 198	3 077	1700
12	$67B_2O_3 \cdot 12Li_2O \cdot 20Cs_2O$	58 309	73 595	2030	9 903	12 142	12 017	6703
13	$67B_2O_3 \cdot 16Li_2O \cdot 16Cs_2O$	32 402	45 316	1117	5 107	6 155	5 941	3247
14	$67B_2O_3 \cdot 20Li_2O \cdot 12Cs_2O$	29 806	40 813	1064	5 147	6 384	6 311	3514
15	$67B_2O_3 \cdot 24Li_2O \cdot 8Cs_2O$	36 871	49 348	1328	6 332	8 120	8 293	4727

transitions. The exponential dependence of the multiphonon relaxation rate W_{MPR} on the energy gap to the next lower level ΔE has been experimentally established for a number of crystals and glasses and is given by [6]

$$W_{MPR} = C \exp[-\alpha \Delta E](n+1)^P \tag{4}$$

where C and α are positive, host dependent constants, which are almost independent of the specific 4f level of trivalent rare earth ions except in a few cases, $n = 1/(\exp(\hbar\omega/KT) - 1)$ and $P = \Delta E/\hbar\omega$ ($\hbar\omega = 1400 \, cm^{-1}$ (for borate glass) and $KT = 209 \, cm^{-1}$). Using the above

Table 4. Branching ratios (β) and integrated absorption cross sections ($\Sigma \times 10^{18}$ cm^{-1}) of certain transitions of Ho^{3+} doped mixed alkali borate glasses.

Sample no	Glass composition	$^3H_5 \to {}^5I_7$ β	Σ	$^5G_6 \to {}^5I_8$ β	Σ	$^3K_8 \to {}^5I_8$ β	Σ	$^5F_4 \to {}^5I_8$ β	Σ	$^5F_5 \to {}^5I_8$ β	Σ
1	67B$_2$O$_3$·8Li$_2$O·24Na$_2$O	0.725	25.8	0.885	47.3	0.880	1.44	0.805	8.90	0.720	6.14
2	67B$_2$O$_3$·12Li$_2$O·20Na$_2$O	0.697	28.2	0.879	52.1	0.881	1.68	0.797	10.87	0.732	7.82
3	67B$_2$O$_3$·16Li$_2$O·16Na$_2$O	0.680	29.4	0.875	54.4	0.882	1.87	0.800	12.45	0.737	8.99
4	67B$_2$O$_3$·20Li$_2$O·12Na$_2$O	0.661	28.6	0.870	53.8	0.882	2.01	0.802	13.75	0.742	9.94
5	67B$_2$O$_3$·24Li$_2$O·8Na$_2$O	0.664	29.6	0.871	55.6	0.882	2.04	0.802	13.91	0.742	10.08
6	67B$_2$O$_3$·8Li$_2$O·24K$_2$O	0.797	15.2	0.904	28.5	0.879	0.69	0.823	3.50	0.690	2.20
7	67B$_2$O$_3$·12Li$_2$O·20K$_2$O	0.767	21.7	0.896	40.1	0.879	1.07	0.812	5.97	0.703	3.94
8	67B$_2$O$_3$·16Li$_2$O·16K$_2$O	0.728	24.7	0.886	44.4	0.879	1.33	0.803	8.11	0.717	5.59
9	67B$_2$O$_3$·20Li$_2$O·12K$_2$O	0.710	22.7	0.883	41.8	0.881	1.31	0.802	8.31	0.728	5.87
10	67B$_2$O$_3$·24Li$_2$O·8K$_2$O	0.676	19.9	0.873	37.8	0.881	1.30	0.794	8.78	0.737	6.64
11	67B$_2$O$_3$·8Li$_2$O·24Cs$_2$O	0.780	16.4	0.902	30.3	0.884	0.67	0.800	3.47	0.711	2.42
12	67B$_2$O$_3$·12Li$_2$O·20Cs$_2$O	0.689	34.6	0.877	63.66	0.881	2.04	0.790	13.35	0.732	9.89
13	67B$_2$O$_3$·16Li$_2$O·16Cs$_2$O	0.733	21.5	0.889	39.33	0.881	1.12	0.803	6.75	0.723	4.72
14	67B$_2$O$_3$·20Li$_2$O·12Cs$_2$O	0.699	18.7	0.878	34.9	0.882	1.07	0.787	7.00	0.730	5.16
15	67B$_2$O$_3$·24Li$_2$O·8Cs$_2$O	0.671	21.9	0.871	41.99	0.883	1.33	0.777	9.10	0.739	7.03

equation, non-radiative relaxation rate constants for the various Ho^{3+} excited states in mixed alkali borate glasses were calculated using the values $\alpha = 3.8 \times 10^{-3}$ cm and $C = 2.9 \times 10^{12}$ s^{-1} reported for borate glasses [25]. The predicted non-radiative relaxation rates for the observed excited state multiplets are presented in table 5 for all the glasses studied. It is observed that non-radiative decay rate is the dominant relaxation process for all the excited states of Ho^{3+} in borate glasses.

3.3. Emission properties

The photoluminescence spectrum of Ho^{3+} recorded under excitation wavelength 418 nm is shown in figure 4 for lithium sodium mixed alkali borate glasses. In the present work, we have not obtained clear emission spectra for the lithium caesium glass matrix, hence we have not studied the emission properties in this glass matrix. In the emission spectra of Ho^{3+}, three transitions $^5F_5 \to {}^5I_8$, $^5F_3 \to {}^5I_8$ and $^3K_8 \to {}^5I_8$ are identified. Among these three transitions, the $^5F_5 \to {}^5I_8$ transition is sharp and the intensity of the transition varies with x in the glass composition. Table 6 gives effective band widths ($\Delta\lambda_p$) and stimulated emission cross sections (σ_p) of the $^5F_5 \to {}^5I_8$ and $^3K_8 \to {}^5I_8$ transitions which are calculated using the expressions given in [26]. From the table it is observed that the stimulated emission cross sections of both the transitions are increasing with the increase of lithium content (i.e. decrease of sodium/potassium content). From the emission spectra it is concluded that among all the mixed alkali borate glasses studied, the glasses with $x = 24$ mol% may be useful for laser excitation as the transitions have higher emission cross sections.

4. Conclusions

Judd–Ofelt theory works well for the Ho^{3+} ion in the mixed alkali borate glasses. The Judd–Ofelt parameter, Ω_2, is greater in mixed alkali borate glasses than in the corresponding binary borate glasses. It indicates higher covalency between holmium cations and oxide anions in mixed alkali borate glasses. There is a shift of peak wavelength of the hypersensitive transition towards longer wavelengths with the increase of x in lithium sodium and lithium potassium

Table 5. Non-radiative relaxation rates (W_{MPR}) (s^{-1}) of certain excited states of Ho^{3+} in mixed alkali borate glasses (ΔE values are in cm^{-1}).

		$^5G_5$		$^5G_6$		$^3K_8$		$^5F_2$		$^5F_3$		$^5F_4$		$^5S_2$	
	Glass	ΔE	W_{MPR}	ΔE	W_{MPR}	ΔE	W_{MPR}	ΔE	W_{MPR}	ΔE	W_{MPR}	ΔE	W_{MPR}	ΔE	W_{MPR}
1	Glass 1	1498	9.79×10^9	1702	4.51×10^9	446	5.33×10^{11}	586	3.13×10^{11}	1950	1.76×10^9	17	2.72×10^{12}	3007	3.17×10^7
2	Glass 2	1548	8.09×10^9	1556	7.85×10^9	329	8.31×10^{11}	585	3.14×10^{11}	1946	1.78×10^9	25	2.64×10^{12}	2985	3.44×10^7
3	Glass 3	1586	7.01×10^9	1492	10.02×10^9	310	8.93×10^{11}	589	3.09×10^{11}	1940	1.82×10^9	33	2.56×10^{12}	2987	3.42×10^7
4	Glass 4	1607	6.47×10^9	1412	13.57×10^9	234	11.92×10^{11}	566	3.38×10^{11}	1948	1.77×10^9	79	2.15×10^{12}	2947	3.98×10^7
5	Glass 5	1607	6.47×10^9	1412	13.57×10^9	234	11.92×10^{11}	566	3.38×10^{11}	1948	1.77×10^9	79	2.15×10^{12}	2947	3.98×10^7
6	Glass 6	1472	10.81×10^9	1769	3.16×10^9	516	4.08×10^{11}	540	3.73×10^{11}	1996	1.48×10^9	42	2.47×10^{12}	2974	3.59×10^7
7	Glass 7	1441	12.16×10^9	1813	2.96×10^9	564	3.78×10^{11}	564	3.40×10^{11}	1950	1.79×10^9	44	2.45×10^{12}	2998	3.28×10^7
8	Glass 8	1523	8.90×10^9	1724	4.15×10^9	544	3.67×10^{11}	636	2.56×10^{11}	1949	1.76×10^9	112	1.89×10^{12}	3103	2.20×10^7
9	Glass 9	1548	8.09×10^9	1589	6.93×10^9	385	6.72×10^{11}	587	3.12×10^{11}	1949	1.76×10^9	1	2.89×10^{12}	3003	3.21×10^7
10	Glass 10	1598	6.70×10^9	1446	11.93×10^9	269	10.44×10^{11}	564	3.40×10^{11}	1967	1.65×10^9	48	2.42×10^{12}	2962	3.76×10^7
11	Glass 11	1448	11.83×10^9	1769	3.58×10^9	437	5.51×10^{11}	523	3.98×10^{11}	1961	1.69×10^9	82	2.12×10^{12}	2925	4.33×10^7
12	Glass 12	1592	6.85×10^9	1551	8.00×10^9	440	5.45×10^{11}	632	2.63×10^{11}	1949	1.76×10^9	76	2.17×10^{12}	2685	10.81×10^7
13	Glass 13	1496	9.86×10^9	1660	5.29×10^9	381	6.82×10^{11}	564	3.40×10^{11}	1949	1.76×10^9	39	2.50×10^{12}	2965	3.72×10^7
14	Glass 14	1500	9.71×10^9	1703	4.49×10^9	468	4.90×10^{11}	568	3.35×10^{11}	1961	1.69×10^9	22	2.67×10^{12}	3009	3.15×10^7
15	Glass 15	1557	7.82×10^9	1600	6.65×10^9	363	7.30×10^{11}	568	3.35×10^{11}	1961	1.69×10^9	60	2.31×10^{12}	2971	3.63×10^7
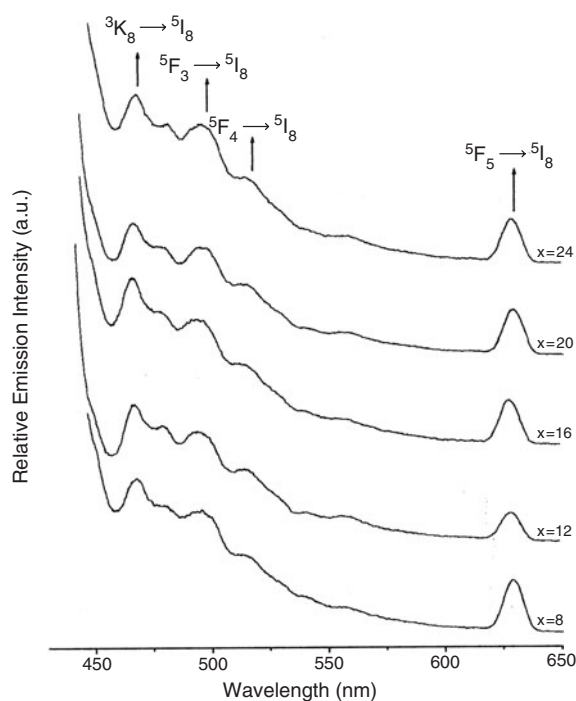
Figure 4. Luminescence spectra of Ho^{3+} in 67B$_2$O$_3$·xLi$_2$O·(32 − x)Na$_2$O glasses.

Table 6. Certain luminescence properties of Ho^{3+} doped mixed alkali borate glasses.

		$^5F_5 \to {}^5I_8$				$^3K_8 \to {}^5I_8$			
Sample no	Glass composition	λ_P (nm)	A_{rad} (s^{-1})	$\Delta\lambda$ (nm)	σ_P (10^{-20} cm^2)	λ_P (nm)	A_{rad} (s^{-1})	$\Delta\lambda$ (nm)	σ_P (10^{-20} cm^2)
1	67B$_2$O$_3$·8Li$_2$O·24Na$_2$O	630.8	3050	9.5	2.49	469.1	1258	8.95	0.33
2	67B$_2$O$_3$·12Li$_2$O·20Na$_2$O	629.4	3873	10.3	2.90	464.7	1479	9.43	0.35
3	67B$_2$O$_3$·16Li$_2$O·16Na$_2$O	628.7	4471	9.5	3.58	466.9	1658	9.70	0.39
4	67B$_2$O$_3$·20Li$_2$O·12Na$_2$O	630.1	4925	10.3	3.70	466.2	1786	8.20	0.50
5	67B$_2$O$_3$·24Li$_2$O·8Na$_2$O	630.1	4986	10.3	3.75	469.8	1813	7.46	0.58
6	67B$_2$O$_3$·8Li$_2$O·24K$_2$O	631.0	1100	10.8	0.79	468.0	595	7.69	0.18
7	67B$_2$O$_3$·12Li$_2$O·20K$_2$O	630.0	1971	10.7	1.41	467.7	923	8.46	0.25
8	67B$_2$O$_3$·16Li$_2$O·16K$_2$O	629.2	2794	10.0	2.14	466.9	1158	9.67	0.27
9	67B$_2$O$_3$·20Li$_2$O·12K$_2$O	628.4	2926	9.2	2.42	468.5	1158	9.23	0.29
10	67B$_2$O$_3$·24Li$_2$O·8K$_2$O	630.0	3187	9.2	2.67	465.2	1157	8.46	0.32

mixed alkali borate glass matrices. The spectral profile of the hypersensitive transition changes with x in lithium sodium, lithium potassium and lithium caesium glasses, which indicates structural changes. From the variation of the sum of the Judd–Ofelt intensity parameters ($\sum \Omega_\lambda$), the position of the peak wavelength of the hypersensitive transition and peak intensity ratios (I_L/I_S), it is observed that covalency increases with the increase of x in the lithium sodium glass matrix. Some structural changes were observed at $x = 20$ and 24 mol% in lithium potassium and lithium caesium glass matrices.

The total radiative transition rates for all the excited states are low at $x = 8$ mol% in all the three mixed alkali borate glasses. These values are high at $x = 24$ and 12 mol% in lithium

sodium and lithium caesium glass matrices. The magnitude of branching ratios are high at $x = 8$ mol% for the $^5G_6 \rightarrow {}^5I_8$ transition in all the three glass matrices and the integrated absorption cross sections are also high for this transition among all the transitions. From the emission spectra, it is concluded that among all the mixed alkali borate glasses studied, the glasses with $x = 24$ mol% may be useful for laser excitation as the transitions $^5F_5 \rightarrow {}^5I_8$ and $^3K_8 \rightarrow {}^5I_8$ have higher emission crosssections.

Acknowledgments

References

[1] Esterocwitz L and Allen R 1989 *Proc. SPIE* **1048** 129
[2] Johnson L F, Guggenheim H G, Rich T C and Ostermayer F W 1972 *J. Appl. Phys.* **43** 1125
[3] Hart D W, Jani M and Barnes N P 1996 *Opt. Lett.* **21** 728
[4] Kaminskii A A, Fedorov V A, Sarkisov S E, Bohm J, Reiche P and Scultze D 1979 *Phys. Status Solidi* a **53** K219
[5] Malinowski M, Frukacz Z, Szuflinska M, Wnukand A and Kaczkan M 2000 *J. Alloys Compounds* **300/301** 389
[6] Shojiya M, Kawamoto Y and Kadono K 2001 *J. Appl. Phys.* **89** 4944
[7] Reddy M R, Raju S B and Veeraiah N 2000 *J. Phys. Chem. Solids* **61** 1567
[8] Ratnakaram Y C, Chakradhar R P S, Ramesh K P, Rao J L and Ramakrishna J 2003 *J. Mater. Sci.* **38** 833
[9] Day D E 1976 *J. Non-Cryst. Solids* **21** 343
[10] Maass P, Bunde A and Ingram M D 1992 *Phys. Rev. Lett.* **68** 3064
[11] Bunde A, Ingram M D and Maass P 1994 *J. Non-Cryst. Solids* **72** 1222
[12] Soppe W, Kleerebezem J and den Hartog H W 1987 *J. Non-Cryst. Solids* **93** 142
[13] Krogh-Moe J 1962 *Phys. Chem. Glasses* **3** 101
[14] Chong B C L, Choo S H, Feller S, Teoh B, Mathews O, Khaw E J, Fel D, Chong K H, Affatigato M, Bain D, Hazen K and Farroqu K 1989 *J. Non-Cryst. Solids* **109** 113
[15] Ratnakaram Y C, Abdul Altaf M D, Chakradhar R P S, Rao J L and Ramakrishna J 2003 *Phys. Status Solidi* b **236** 200
[16] Carnall W T, Goodman G L, Rajnak K and Rana R S 1988 A systematic analysis of the spectra of the lanthanides doped into single crystal LaF$_3$ *Report* ANL-88-8, Chemistry division, Argonne National Laboratory, Argonne, IL
[17] Judd B R 1962 *Phys. Rev.* **127** 750
[18] Ofelt G S 1962 *J. Chem. Phys.* **37** 511
[19] Reisfed R 1975 *Structure and Bonding* ed J D Duni *et al* (Berlin: Springer)
[20] Jorgensen C K 1971 *Modern Aspects of Ligand Field Theory* (Amsterdam: North-Holland)
[21] Carnall W T, Crosswhite H and Crosswhite H M 1977 Energy level structure and transition probabilities for trivalent lanthanides in LaF$_3$ *Argonne National Laboratory Report* Argonne National Laboratory, Argonne, IL
[22] Saisudha M B and Ramakrishna J 1996 *Phys. Rev.* B **53** 6186
[23] Oomen E W J L and van Dongen A M A 1989 *J. Non-Cryst. Solids* **111** 205
[24] Rawson H 1967 *Inorganic Glass Forming Systems* (London: Academic)
[25] Shojiya M, Takahashi M, Kanno R, Kawamoto Y and Kadono K 1997 *J. Appl. Phys.* **82** 6259
[26] Saisudha M B, Koteswara Rao K S R, Bhat H L and Ramakrishna J 1996 *J. Appl. Phys.* **80** 4845
[27] Takebe H, Nageno Y and Morinaga K 1995 *J. Am. Chem. Soc.* **78** 116
     Takebe H, Nageno Y and Morinaga K 1995 *J. Am. Chem. Soc.* **78** 2287